



**HAL**  
open science

## The European ITER Test Blanket Modules: Assessment of manufacturing technologies for HCLL

L. Forest, J. Tosi, A. Li Puma, O. Doyen, N. Thomas, M. Simon-Perret, M. Zmitko

► **To cite this version:**

L. Forest, J. Tosi, A. Li Puma, O. Doyen, N. Thomas, et al.. The European ITER Test Blanket Modules: Assessment of manufacturing technologies for HCLL. ISFNT-13, Sep 2017, Kyoto, Japan. cea-02434528

**HAL Id: cea-02434528**

**<https://cea.hal.science/cea-02434528v1>**

Submitted on 10 Jan 2020

**HAL** is a multi-disciplinary open access archive for the deposit and dissemination of scientific research documents, whether they are published or not. The documents may come from teaching and research institutions in France or abroad, or from public or private research centers.

L'archive ouverte pluridisciplinaire **HAL**, est destinée au dépôt et à la diffusion de documents scientifiques de niveau recherche, publiés ou non, émanant des établissements d'enseignement et de recherche français ou étrangers, des laboratoires publics ou privés.

# The European ITER Test Blanket Modules: Assessment of manufacturing technologies for HCLL

Laurent FOREST<sup>a\*</sup>, Jérôme TOSI<sup>a</sup>, Antonella Li PUMA<sup>a</sup>, Olivier DOYEN<sup>a</sup>, Noel THOMAS<sup>b</sup>, Melchior SIMON-PERRET<sup>b</sup>, Milan ZMITKO<sup>c</sup>

<sup>a</sup>*DEN-Service d'Etudes Mécaniques et Thermiques (SEMT), CEA, Université Paris-Saclay, F-91191 Gif sur Yvette, France*

<sup>b</sup>*ATMOSTAT, F-94815 Villejuif, France.*

<sup>c</sup>*Fusion for Energy (F4E), Josep Pla 2, Barcelona, Spain.*

*\*Corresponding author: laurent.forest@cea.fr*

The HCLL-TBM (Helium Cooled Lithium Lead Test Blanket Module) is one of the two European TBMs chosen to be tested in ITER. HCLL TBM structure is constituted by a box, made of two Side Caps (SCs) and a First Wall (FW), stiffened by horizontal and vertical Stiffening Plates (SP) and closed on its back by several back plates (BPs). All structure subcomponents are internally cooled by Helium circulating in meandering squared section channels. This paper describes manufacturing technologies developed and implemented to assemble the SPs into the box.

It presents the preliminary manufacturing procedure developed and applied for the assembly of the SPs into the box by Tungsten Inert Gas (TIG). Several mock ups have been manufactured from laboratory to feasibility mock ups (scale 1:1) on which non-destructive and destructive tests have been carried-out to identify the preliminary manufacturing procedure. Due to TBM specificities (namely complex welding trajectories, heavy and big components, plates with channels, space constraints, ...) a specific welding facility including a custom welding torch and an automated bench has been achieved and is also described in the paper.

We detail the adopted manufacturing strategies, as the optimization of welding sequence to minimize distortions and the customization of welding parameters, to compensate machining tolerances and welding gaps. Results such as welded joints quality and microstructure, internal cooling channel deformation and structure distortions are reported. These developments have been performed following a standardized procedure complying with professional codes and standards (RCC-MRx).

Keywords: ITER, Test Blanket Module, manufacturing, welding, specification.

## 1 Introduction

Europe is currently developing several breeder blanket concepts for future thermonuclear DEMONstration fusion reactors [1]. Two concepts have been chosen to be tested in ITER under the form of Test Blanket Modules (TBMs) [2]: the Helium-Cooled Lithium-Lead (HCLL, Figure 1a) concept which uses the eutectic Pb-15.7Li (enriched in <sup>6</sup>Li) as both tritium breeder and neutron multiplier and the Helium-Cooled Pebble-Bed (HCPB) concept with lithiated ceramic (enriched in <sup>6</sup>Li) pebbles as tritium breeder and beryllium pebbles as neutron multiplier. Both European TBMs designs share similar steel box structure of 1670 (poloidal) x 462 (toroidal) x 685mm (radial) overall dimensions which is formed by a U-shaped curved plate called First Wall (FW), closed on its sides by Side Caps (SC) and in the rear by a set of parallel plates assembled together and forming a coolant manifold system for the pressurized Helium coolant flow distribution. Internally, the steel box is stiffened by horizontal and vertical stiffening plates (SP) constituting the Stiffening Grid (SG). This grid, whose main function is to withstand an in-box accidental over-pressurization, defines an array of internal cells where specific breeding components called Breeder Units (BU) are inserted.

EUROFER97 steel (X10CrWVTa9-1), a reduced activation ferritic-martensitic (RAFM) steel, specially developed in EU for fusion reactors, is used as structural material. EUROFER97 is derived from the conventional 9Cr-1Mo steel, with the high activation elements (Mo, Nb, Ni, Cu and N) either replaced by equivalent low activation

elements (e.g. W, V and Ta) or reduced to the lowest content that is technically achievable at reasonable cost. Main advantages of RAFM steel over austenitic stainless steels are related to their excellent dimensional stability (low creep and swelling) under neutron irradiation as well as higher performance and compatibility with breeding materials and coolants. Both concepts use pressurized helium as coolant for efficient heat extraction (300-500 °C, 8 MPa).

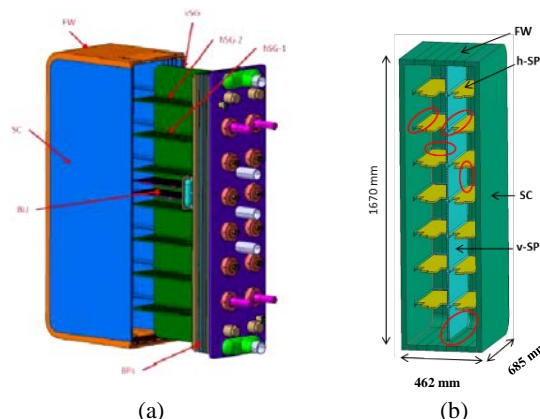


Figure 1: Exploded view of the HCLL TBM steel structure [2]

Each EU TBM is a multi-chamber box structure made of plates cooled by multiple meandering channels where circulates the pressurized helium.

Specific technologies and procedures have been developed and implemented in the frame of the EU framework

contract to manufacture TBM sub-components (Figure 1a) namely CPs, SPs, SC, FW. They are based on fusion and diffusion welding techniques taking into account specificities of the EUROFER97 steel [3].

Next step in the TBM manufacturing sequence is the assembly by welding of these sub-components, namely of the SPs (one vertical, vSP and fourteen horizontal, hSP) into the box constituted by the FW and SC (Figure 1b), assembly which features several challenges. Numerous welds are indeed needed to assembly the SG into the box. Cooling channels are embedded in the plates at  $\sim 5$  mm from the welded joint. Damage or deformation of the cooling channels shall be avoided. Welding of plates (thickness of 11 mm for vSP and 30 mm for the box) weakened by inner channels into the large TBM (fig.1a) exacerbates the sensitivity to welding distortions which can be an issue regarding the assembly feasibility and compliance with geometric tolerances. In this frame this paper describes studies carried out to define the welding process and to develop the preliminary welding procedure to realize this assembly.

A first assessment was carried out to identify candidate welding processes, two of which were retained as the most promising (laser and Gas Tungsten Arc Welding (GTAW)). The GTAW using filler material is the reference process. A specific robotic installation has been specified and procured which is described in section 2.

Section 3 describes the methodology and mock ups design. Performed tests and results are reported in section 4 where the quality of welds is assessed with regard to assumed standards and French nuclear code (RCC-MRx [4]). Main conclusions are given in section 5.

## 2 Welding facility

The complex structure of the SG, featuring, amongst other, low accessibility and long welded length (125 m in total), has required to design and procure a specific robotic welding installation (see Figure 2).

This equipment consists of a welding head driven by a robot allowing its displacement along six axes and a manipulator moving the TBM and its clamping system (about 1300 kg) along three axes (two rotations and one translation). The entire robotic installation (including TBM) has a mass of around seven tons. Due to the geometry of the TBM, special attention has been paid to the development of the GTAW welding torch. The head is mounted on a 2 m long arm featuring a  $90^\circ$  angle or a straight arm, dedicated respectively for the welding of vSP and hSPs (see red zones on Figure 1b). Both solutions allow keeping the same torch angle position and keeping the filler wire always before the torch. Indeed, trajectories for vSP welding consists of both straight (TBM bottom, top and back) and rounded parts (TBM corners). Dimensions of the arm have been minimized to allow the access to the welding grooves inside the TBM especially for the welding of hSPs. The automation of the process and its robotization enable the precision required for the positioning of the GTAW torch in the chamfer and improve the repeatability of the operations and the robustness of the process.

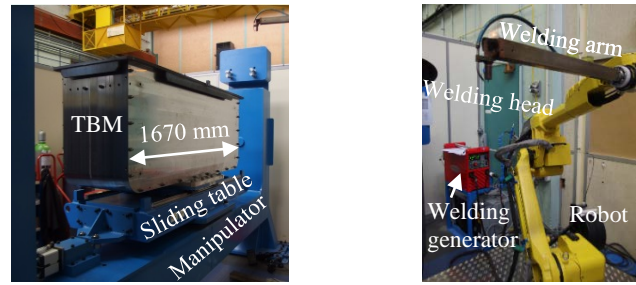


Figure 2: GTAW facility

## 3 Methodology and mock ups

The methodology is based on using mock ups of increasing representativeness. Preliminary welding procedures are developed on "laboratory" mock-ups (LMUs) and then their applicability/transferability to a full scale component is investigated on Intermediate Mock Ups (IMUs) and then validated on a Feasibility Mock-Up (FMU). LMUs do not take into account the real heat pumping of the full scale components which is more important. Nevertheless, they enable to preliminarily make out a weldability domain which will be transferred and adapted in the next step on full scale component (IMUs and FMU). Objectives of tests conducted on LMUs are in other words to find welding parameters guaranteeing a good weld quality. Both Non Destructive Test (NDT, X-rays) and metallographic inspections on cross sections are used to assess weld quality.

Two kinds of LMUs have been used to investigate various situations present in the TBM. The first type consists of a 300 mm long and 11 mm thick plate with several start and stop zones, in order to find the welding parameters for the beginning and for the end of the welds (Figure 3a). On each LMU (Figure 3a), three different chamfers are machined. The second LMU type, shown in Figure 3b, is used to represent straight and round parts. In the Figure 3b, the chosen chamfer geometry can be observed. A double U-geometry chamfer has been selected to minimize distortions induced by the welding operations

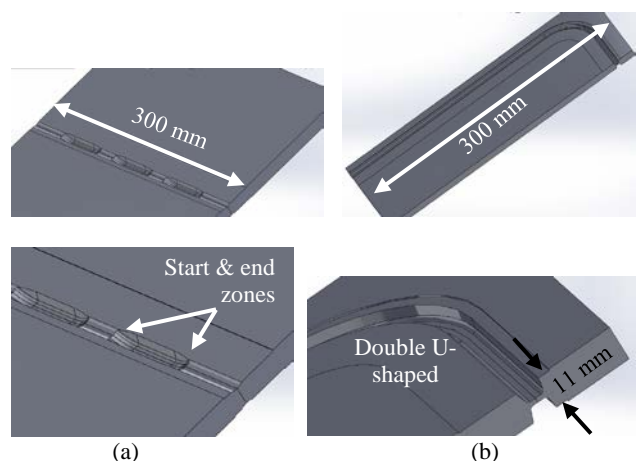


Figure 3: geometries of LMUs. (a) start and end zones, (b) curved LMU

Concerning IMUs and FMU mock-ups, they consist of a box in which SPs are welded. The box and the SPs feature same dimensions as in the TBM (Figure 1b). Straight channels have been drilled into the vSP in order to be representative of real component stiffness. Indeed, the vSP



is the most likely to distort during its welding compare to the thick FW. The TBM box (Figure 4c) is a mechanical assembly of 2 side caps (Figure 4b), 6 U-shape standard parts and 1 U-shape central part (Figure 4a). During the welding of vSP, the mock-up clamping is ensured by refractory metal frame and struts (Figure 5).

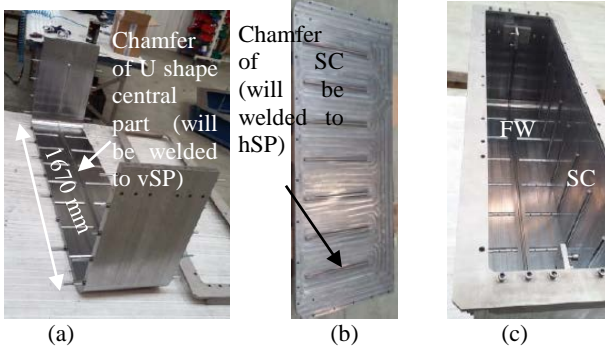


Figure 4: mechanical assembly of TBM box

All horizontal stiffening plates have been machined and custom-made taking into account the measured distortion of the vSP after welding and post welding heat treatment. The main difficulty is to be able to insert all hSPs into the box after vSP welding; once all hSPs are inserted and clamped, no major distortion should occur during hSPs welding.

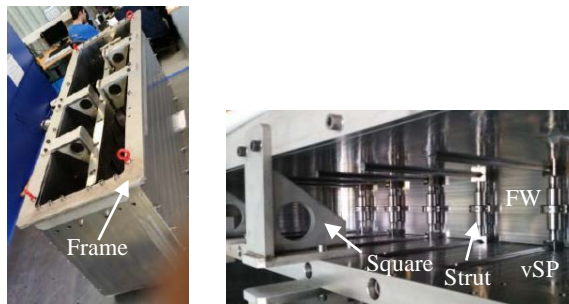


Figure 5: TBM box assembly with vSP and clamping tools

#### 4 Welding tests and main results

P91 steel (X10CrMoVNb9-1) is used as materials for all mock ups. This off-the-shelf material is simpler to procure and its weldability behavior is very similar to EUROFER97. The welding filler metal (diameter of 1.2 mm) is a 9%Cr steel recommended for P91 steel. Automatic GTAW process is performed in flat position. Welding parameters are selected in a way to guarantee a good robustness. Repairing procedures are also defined by using the same equipment, as far as possible.

##### 4.1 LMUs

Several tests have been carried out varying: welding speed, current mode (continuous & pulsed), frequency, hot and cool times, high & low intensity, wire feed rate, voltage, position of filler wire and electrode in the chamfer, wire guide, shielding flowrate and nature (Ar and Ar/He). Adding of He in gas shielding, characterized by a higher ionization potential than Ar, allows improving the thermal conductivity of the arc, a more uniform heat distribution and the wettability of the weld pool. Main consequence is the minimization of welding defects as lack of fusion. Schematic view of pulsed current and filler wire speed are presented in Figure 6.

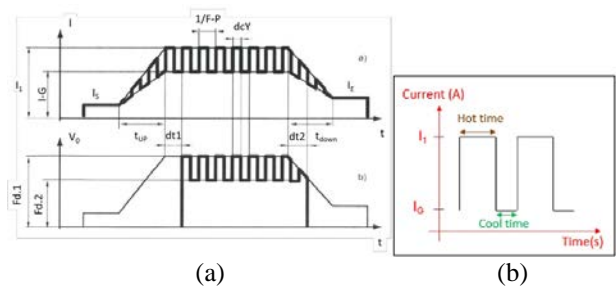


Figure 6: schematic view of current (a) and filler wire speed (b), as detailed in the notice of the power source (IS: start current, I1: high current, IG: low current, IE: end current, dSL: down slope time, tE: time end)

In order to keep constant the welding energy during the different welding phases, voltage is kept constant by using the Automatic Voltage Constant system.

The main welding sequence is presented in Figure 7. Cleaning phases are performed before and after each pass with ethanol. To remove the light oxidation, a brushing step is realized after each run. Tack welding, is realized at first with four dashes of about 15 mm length. After each run, the weld quality is checked by visual inspection. After welding, a Post Welding Heat Treatment (PWHT) can be performed (depending on the objectives of the test). Analysis includes NDT (X-rays) and observations with an optical microscope on cross sections to characterize the weld quality.

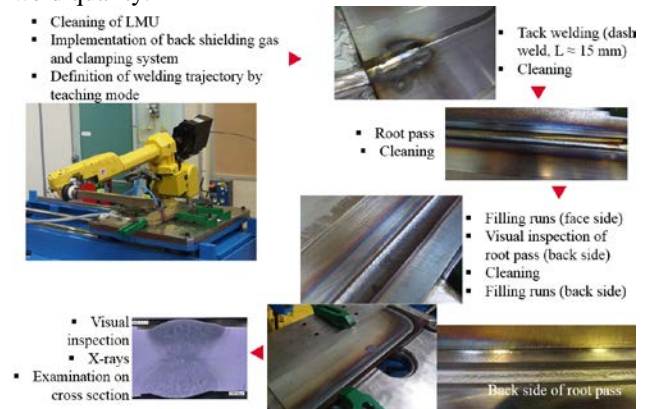


Figure 7: main welding steps on LMU

Based on literature [5] and on our feedback, a PWHT is performed at 760°C under air atmosphere, to soft martensite in the Welded Zone (WZ) and in the Heat Affected Zone (HAZ) and to recover mechanical properties (e.g elongation and ultimate tensile strength). Impact of PWHT on welded microstructures is shown in Figure 8a and is appreciated by Vickers hardness filiations and mapping performed with a weight of 1kg and located at mid thickness (Figure 8b).

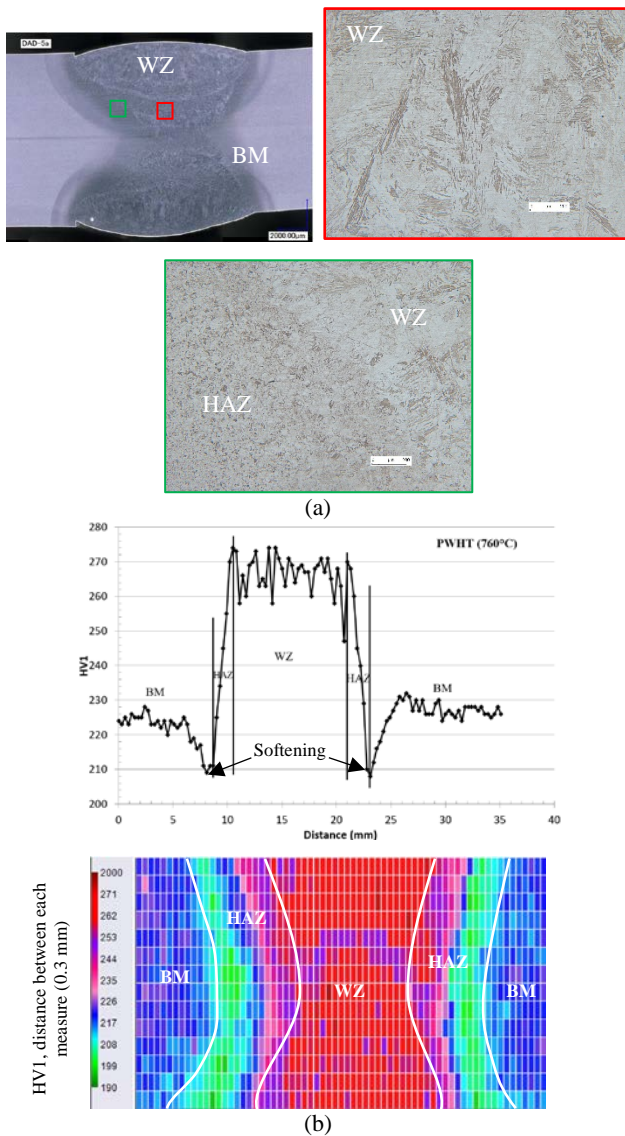
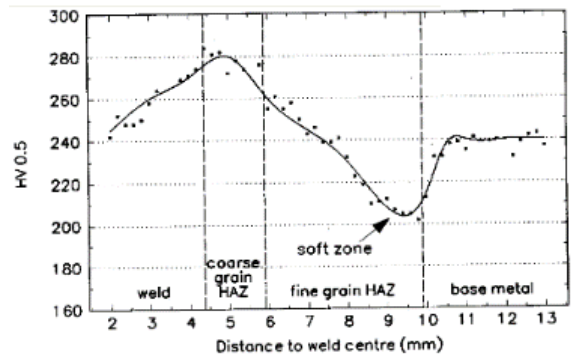


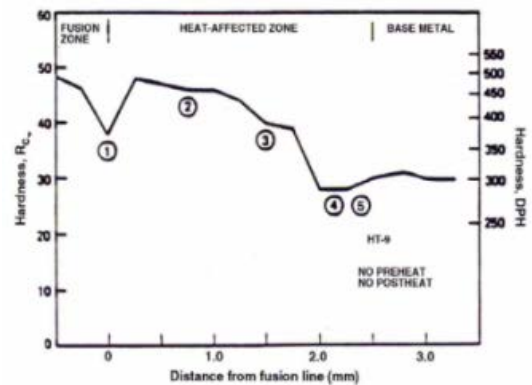
Figure 8: metallographic examination on a LMU weld cross sections after PWHT. (a) optical microscope, (b) hardness measurement

After welding, as Base Metal (BM) is delivered quenched and tempered, an over-ageing effect is created in the extreme HAZ, in the area close to the BM (Figure 8a). This over-ageing effect leads to a much localized reduction of hardness in this area (Figure 9, [5]). This softening is rather limited in terms of width and it will normally not affect the transversal tensile properties of the assembly. However, this softening has an impact on the assembly's creep strength [6].

Figure 9b [7] shows relations between metallurgical state of 9% Cr steel welds with reached temperatures during the welding and the hardnesses. The observed HAZ softening (Figure 8b), about 20 Vickers points near the BM and 2.5 mm width, is consistent with the data given in the literature [5].



(a)



Heat - Affected - Zone (HAZ) [as-welded]:

- Region 1  $T_m > T > T_{\gamma\delta}$   $\gamma + \delta \rightarrow$  Martensite +  $\delta$
- Region 2  $T_{\gamma\delta} > T > A_{c3}$  Coarse grained  $\gamma \rightarrow$  Martensite
- Region 3  $T_{\gamma} > T > A_{c3}$  Fine grained  $\gamma \rightarrow$  Martensite
- Region 4  $A_{c3} > T > A_{c1}$   $\gamma \rightarrow$  Martensite + Overtempered Martensite
- Region 5  $A_{c1} > T > T_T$  Overtempered Martensite

(b)

Figure 9: (a) hardness profile after PWHT through a P91 welded joint [5], (b) correlation between welded microstructure, maximum temperature and hardness value [7]

The weld zone characterized after PWHT, shown in Figure 8a, is a tempered martensitic and microalloyed. These observations are consistent with metallurgical structure assessed by means of a diagram defined for ferritic and/or martensitic stainless steels by Balmforth and Lippold [8] (Figure 10).

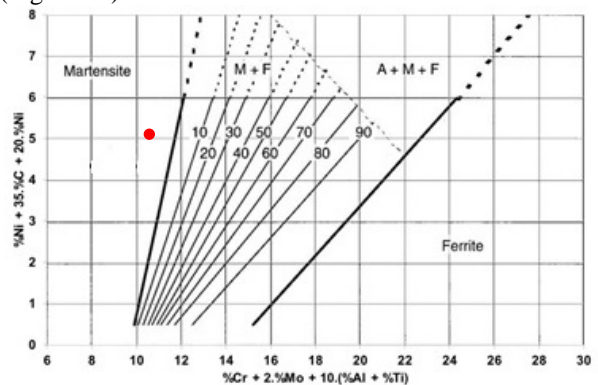


Figure 10: prediction of 9Cr steel structure of the weld metal zone [8]

Although this diagram is specific to stainless steels (its field of application is given for grades with a chromium content exceeding 11%), it was designed also on martensitic grades with 9% chromium, which means that it can be considered as applicable. The structure of the weld metal zone, without filler metal, after cooling at ambient



temperature, will be completely martensitic (see red point for tested material in the Figure 10).

On the basis of these welding tests and the results of the non-destructive and destructive examinations, a first weldability domain is defined in continuous and pulsed currents. Good welded quality is ensured with a maximum permissible gap between the plates to weld of 0.5 mm.

It has to be noted that no preheating was done and inter pass temperatures are applied as preconized to prevent cold cracking on of the metallurgical risks identified on 9%Cr steel welds. This phenomenon is related to three parameters as diffusible hydrogen content (parameter very dependent of welding process and its implementation; to minimize H content allows to reduce this sensitivity), stress induced by the welding operation (to minimize it is favorable to decrease cold cracking sensitivity) and solidification structure (in our case, EUROFER97 has a hard martensite structure [8]). Preheating and post heating treatment favor the diffusion of hydrogen and allows therefore to reduce this risk. Specific welding tests [9], performed with GTAW process and not detailed in this paper, revealed the very low risk for EUROFER97 steels.

#### 4.2 IMUs

Two IMUs have been realized, one constituted by the vSP welded on the box and one featuring the vSP and height hSP.

Due to dimensional tolerances after machining and distortion after welding, different according to the size of the components to be welded, the operating weldability domain developed on LMU has needed to be enriched on full scale component to compensate, among other, important gap (up to 1.5 mm) between the elements to be welded (Figure 11). Operating strategies are implemented such as the welding current pulsation aiming to better manage the deposited energy and to avoid weld pool collapses and a weaving function of the welding torch.

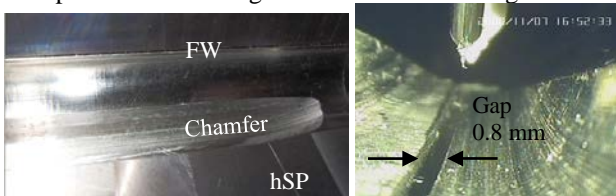


Figure 11: examples of chamfer before welding (a) without gap and (b) with gap

At most, eight passes are required to fill the chamfer in double U-shaped of thickness 11mm and 360 passes are needed for the assembly of the full scale component. Figure 12 shows main types of welding passes, namely the most critical root pass (because of a risk of burn through and a repair difficult to implement), the support pass and the filling passes presenting higher deposition rates and higher energies.



Figure 12: runs welding sequence

Each pass is characterized, as already mentioned, by numerous parameters such as, for the main, welding

speed, high and low current, voltage, high and low wire feed rate, frequency, balance of hot and cold currents, dwell time on each end point of sweeping... Tests have highlighted the sensitivity of the positions of the welding wire and the GTAW torch with respect to the chamfer on the weld quality. The positioning is realized via an endoscope for constraint reason.

Another issue revealed during IMU welding is the deviations of weld pool due to the magnetic properties of the 9% Cr steel and the edge effects. A step of degaussing, prior to welding, is then defined to minimize a part of the deviation.

The defined weldability domain takes into account the existence of type defects e.g. burn through and lack of fusion and the implementation of repairs with the same welding installation.

#### 4.3 FMU

Developments on LMUs and IMUs resulted in the assembly of a FMU composed of full scale elements, the box with the vertical plate (vSP) and fourteen hSPs. It should be noted that the welding sequence applied to the FMU is also based on numerical works aimed at minimizing the welding distortions [10]. Positioning, adjustments and welding of the vSP and hSPs are respectively shown in Figure 13a and Figure 13b.

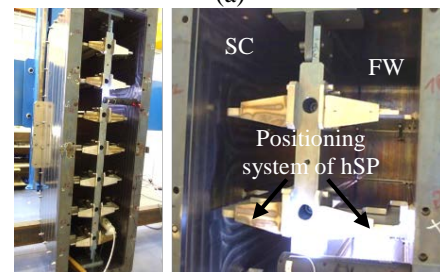
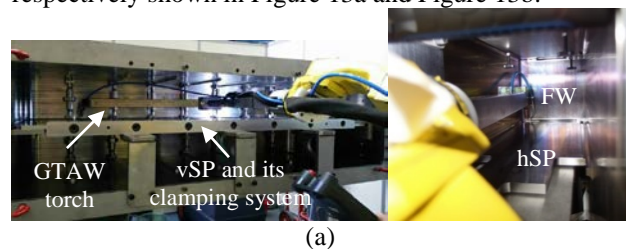


Figure 13: positioning, adjustment and welding of the vSP (a) and hSPs (b)

Two PWHT at 760 °C have been applied, one after the welding of the vSP (to avoid weakening the freshly melted zone when welding the hSPs) and one after the complete welding of the box.

Visual examinations after welding (Figure 14) reveal a good welded quality and are in compliance with the recommendations of the RCC-MRx code [4].

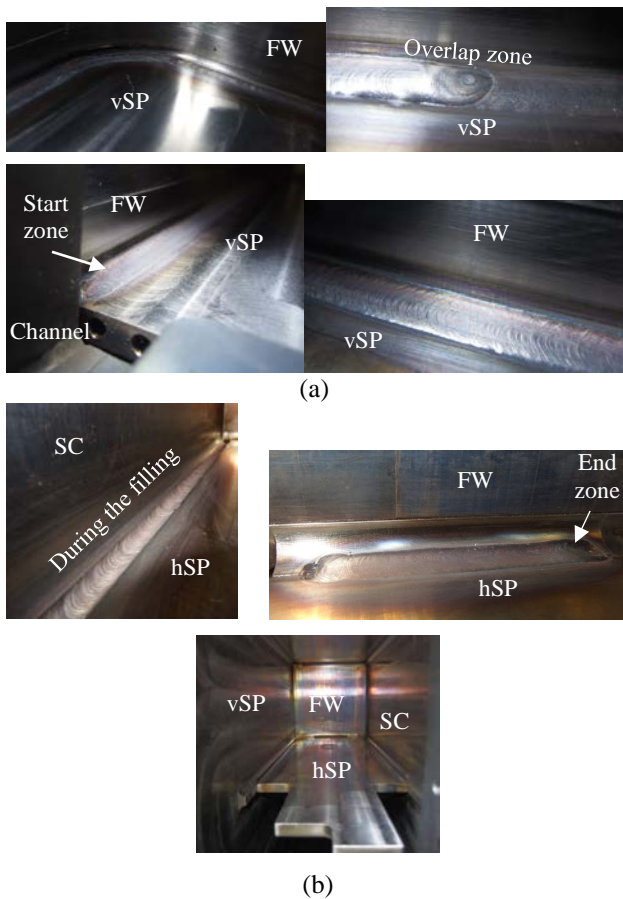


Figure 14: visual inspection of FMU on vSp after welding (a) and hSPs during and after welding (b)

The dimensional controls reveal values on the welded vSP plate that are less than the maximum allowed flatness defect in the toroidal direction  $\pm 2$  mm. Destructive examinations after heat treatment reveal overall a good compactness of the weld (Figure 15a). Nonetheless, small lacks of side-wall fusion (Figure 15b) of dimension up to 1 mm in width have been detected, revealing that implemented welding procedure needs to be reinforced and secured. Microstructure analysis of the WZ and HAZ are conform with observations detailed on LMU.

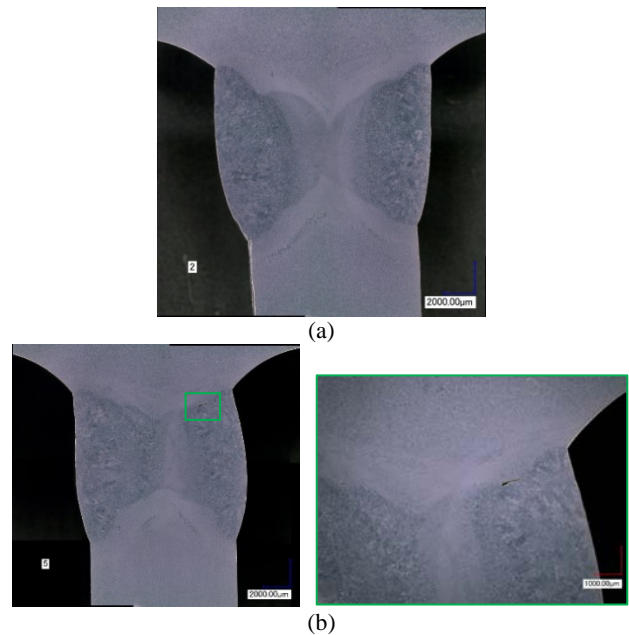


Figure 15: metallographic examination on cross sections. (a) without defect, (b) lack sidewall fusion

## 5 Conclusion

This paper describes the work performed to identify preliminary welding procedures for the assembly of the stiffening grid into the EU TBM box. The complex structure of the SG, composed of the hSP and vSP, and the long welded length required specifying and purchasing a GTAW robotic welding installation including the design and manufacturing of a specific welding torch to reach the less accessible areas. Definition of a preliminary Welding Procedure Specification needs the design and the manufacturing of different kinds of mock-ups as LMUs of increasing representativeness from small plate mock ups to full scale FMU. A double U-shaped geometry chamfer was selected to minimize distortions induced by the welding operations. Welding tests on LMUs and subsequent non-destructive and destructive examinations have allowed to preliminarily identify a weldability domain to ensure good welded quality with a maximum permissible gap between the plates to weld of 0.5 mm. Parameters of PWHT are also defined on LMUs. The resulting microstructure of the welded zone is a tempered martensitic and microalloyed and is consistent with literature. Due to dimensional tolerances after machining and distortions after welding, which are more important on full scale component, the operating weldability domain developed on LMUs has needed to be enriched on full scale components (IMUs) to compensate, among other, important gap (1.5 mm) between the elements to be welded. Operating strategies are implemented such as the welding current pulsation aiming at better managing the deposited energy and to avoid weld pool collapses. A weaving of the welding torch has also been applied. These developments resulted finally in the assembly of a Feasibility Mock-Up, composed of full scale elements: the box with the 1.6 m high vSP and fourteen hSPs. A specific attention has been paid on the welding sequence to minimize distortions. The dimensional controls reveal values on the welded vSP plate that are less than the maximum tolerated flatness defect in

the toroidal direction, i.e.  $< \pm 2$  mm. Destructive tests on FMU reveal overall a good compactness of the weld except sometimes the presence of small lacks of side-wall fusion implying that welding procedures need to be furthermore optimised, i.e. their margins and robustness increased.

### Acknowledgments

This work was performed by ATMOSTAT (ALCEN group) and CEA (at the Nuclear Energy Division, DEN of Saclay) within the framework of Fusion for Energy (F4E) specific contract F4E-OMF-331-05-01-02 concerning the development of the TBM's manufacturing procedures. The views expressed in this publication are the sole responsibility of the authors and do not necessarily reflect the views of the Fusion for Energy and the ITER Organization. Neither Fusion for Energy nor any person acting on behalf of Fusion for Energy is responsible for the use, which might be made of the information in this publication.

### References

- [1] G. Federici et al., «Overview of the design approach and prioritization of R&D activities,» *Fusion Engineering and Design*, pp. 1464-1474, 2016.
- [2] L. Boccaccini, A. Aiello, O. Bedec, F. Cismondi, L. Kosek, T. Ilkei et J.-F. Salavy, «Present status of the conceptual design of the EU test blanket systems,» *Fusion Engineering and Design*, vol. 86, pp. 478-483, 2011.
- [3] M. Zmitko, J. Galabert, N. Thomas, L. Forest, P. Bucci, L. Cogneau, H. Neuberger, J. Rey et Y. Poitevin, «The European ITER Test Blanket Modules: Current status of fabrication technologies development and a way forward,» *Fusion Engineering and Design*, pp. 199-207, 2015.
- [4] AFCEN, «RCC-MRx - Design and construction rules for mechanical components of nuclear installations applicable to high temperature structures and to the ITER vacuum vessel,» 2012.
- [5] W. F. Newell, «Guideline for Welding P(T) 91,» Euroweld Ltd, 2001.
- [6] D. Richardot, J. Vaillant, A. Arbab et W. Bendick, «The T92/P92 Book,» Vallourec & Mannesmann Tubes, 2000.
- [7] R. L. Klueh et D. R. Harries, High-Chromium Ferritic and Martensitic Steels for Nuclear Applications, ASTM, West Conshohocken, PA 19428-2959, 2001.
- [8] M. Balmforth et J. Lippold, «A new ferritic-martensitic stainless steel constitution diagram,» *Welding Journal*, vol. 79, n° 112, pp. 339s-345s, Décembre 2000.
- [9] *Standard NF EN ISO 17642-2 : Destructive tests on welds in metallic materials - cold cracking tests for weldments - Arc welding processes - Part 2: Self-restraint tests*, July 2005.
- [10] O. Doyen, N. Rizzo, L. Forest, J. Tosi, N. Thomas et M. Zmitko, «Assessment of HCLL-TBM optimum welding sequence scenario to minimize welding distortions,» *Fusion Engineering and Design*, vol. 121, pp. 80-86, 2017, In press.